Journal of Thermal Science

https://doi.org/10.1007/s11630-023-1738-6

Prime Mover Capacity Optimization and Thermodynamic Performance Analysis of Internal Combustion Engine Based CCHP System

WANG Shucheng[1], MUHAMMAD Imran[2], LI Hongwei[1], CHEN Xiaoxu[3], QIN Mei[1*]

1. School of Energy and Power Engineering, Northeast Electric Power University, Jilin 132012, China
2. College of Engineering and Physical Sciences, Mechanical, Biomedical and Design Engineering, Aston University, Birmingham B4 7ET, UK
3. Northeast Electric Power Design Institute Co., Ltd. of China Power Engineering Consulting Group, Changchun 130021, China

Abstract: In this research, a solar hybrid combined cooling heating and power (CCHP) system is proposed considering the different scenarios of Prime Movers (PMs) and the part-load performance of PMs is validated by the designed values from the manufacturer of Volvo. Moreover, a multi-optimization model based on a genetic algorithm is developed in order to select both the most promising performance PM and the most cost-effectiveness, environmentally friendly number of collectors for the proposed CCHP system, simultaneously. Then the hourly performance of this solar hybrid CCHP is determined through a case study of a hotel in Shanghai. Results show that the highest efficiency of the PM with larger capacity has the most promising performance and the collector number of 90 turns out to be a superior value for the hotel building based on the primary energy saving ratio of 61.61%. Moreover, on a typical summer day, the recovered waste heat and the solar energy can provide all the thermal energy demands, while, an auxiliary boiler should be started to fulfill the energy gap in both typical transition and winter days. From the simulation result, the CO_2 emissions can be reduced by 856.2 t/a due to the solar energy introduced into the system. Besides, the dynamic investment payback period will change from 3.01 years to 3.56 years when the fuel price (P_{fuel}) ranges from $0.8P_{fuel}$ to$1.2P_{fuel}$.

Keywords: combined cooling heating and power (CCHP) system, distributed energy system, optimization, waste heat recovery, ICE

1. Introduction

Combined cooling heating and power (CCHP) systems are identified as the methods to alleviate the current serious environmental problems. The CCHP systems can significantly reduce SO_2, NO_x, and particulate matter emissions, while the integrated renewable energy technologies, such as distributed photovoltaics, parabolic trough collectors (PTCs), and wind energy, have zero emissions [1–3]. By recovering the waste heat from prime movers (PMs), the thermal efficiency of CCHPs can further be improved, thus reducing fossil fuel consumption [4, 5].

Researchers introduced CCHP systems with a single PM scheme at different running strategies that follow the electric load (FEL) or that follow the thermal load

Received: Aug 05, 2021
AE: GUO Shaopeng
Corresponding author: QIN Mei
E-mail: mq@neepu.edu.cn

Nomenclature

A	Area of single solar collector/m^2	PEC	Primary energy consumption/$kg \cdot s^{-1}$
AB	Auxiliary boiler	PM	Prime mover
AC	Absorption chiller	PTC	Parabolic trough collectors
ATC	Annual total cost/USD	$\dot{Q}_B$	Energy produced by the boiler/kW
CCHP	Combined cooling heating and power	$\dot{Q}_C$	Cooling load/kW
CE	Carbon dioxide emission/$kg \cdot s^{-1}$	$\dot{Q}_C^r$	Recovered energy by the absorption chiller/kW
CESR	Carbon dioxide emissions saving ratio/%	$\dot{Q}_E$	Stored excess energy in TES/kW
COP	Coefficient of performance	$\dot{Q}_H$	Heating load/kW
CP	Critical point	$\dot{Q}_i$	Incident solar energy/kW
DNI	Direct normal irradiance/$W \cdot m^{-2}$	$\dot{Q}_L$	Energy loss/kW
$\dot{E}_B$	Electricity demand/kW	$\dot{Q}_{PM}$	Energy released by fuel combustion/kW
$\dot{E}_G$	Electricity obtained from the power grid/kW	$\dot{Q}_{PTC}$	Produced energy by PTC/kW
$\dot{E}_{PM}$	Electricity generated by PM/kW	$\dot{Q}_S$	Absorbed solar energy/kW
FEL	Follow the electric load	$\dot{Q}_{TES}$	Released energy from TES/kW
FESR	Fuel energy saving ratio/%	$\dot{Q}_W$	Recovered waste heat from PM/kW
i	Interest rate/%	TES	Thermal energy storage
ICE	Internal combustion engines	$\dot{W}$	The rated output power/kW
$K(\theta)$	Incident angle modifier	η_B	Boiler efficiency/%
LHV	Lower heating value of the fuel/$kJ \cdot kg^{-1}$	η_{PM}	Power generation efficiency of PM/%
$\dot{m}_B$	Fuel consumption by the boiler/$kg \cdot s^{-1}$	η_{PTC}	Optical efficiency of collector/%
$\dot{m}_f$	The fuel consumption rate of PM/$kg \cdot s^{-1}$	η_T	Thermal efficiency of the PM/%
N	Number of collectors	θ	Incident angle of solar energy/(°)

(FTL) [6]. They proved that the CCHP systems are more competitive than the separated systems. Moreover, the researchers had investigated the performance of CCHP for different PMs. And the PMs indicated a tendency toward the internal combustion engines (ICEs), gas turbines and fuel cells [7–10].

Roman and Alvery [10] compared the selected PMs, like ICE, micro-turbine, and fuel cell in different climate zones. Results revealed that the ICE showed the best emissions reduction and economic performance. They also suggested that it was necessary to further study a real CCHP system with the right PM. Ebrahimi and Keshavarz [11] used multi-criteria decision-making algorithms to select the best PM for a residential CCHP system under five different climates. Additionally, all the decision-making methods proposed that the ICE was the best PM for the CCHP system. The results indicated that climate differences have changed both the technical magnitude indexes and evaluation indexes, but ultimately decided to remain unchanged under all climatic conditions. Abbasi et al. [12] proposed an innovative procedure to optimize and deployed a residential CCHP system. The multi-objective optimizations based on 3E methods were used to compare different PMs' performance. They concluded that the ICE-based CCHP system showed the most beneficial alternative at all simulated conditions.

Solar energy can significantly reduce fossil fuel consumption in CCHP systems and it will be overwhelmingly environmentally friendly. Su et al. [13] investigated a novel solar hybrid CCHP system under the FEL strategy. Results showed that the total fossil fuel saving ratio reached 3.3% and the annual power-saving ratio got to 77.84%. Yousefi et al. [14] compared two models of CCHP systems using a multi-objective optimization approach. Results revealed that the solar-assisted ICE-based CCHP system had a considerably excellent performance in energy saving and emissions reduction than the conventional CCHP system. Fani and Sadreddin [15] hourly studied a solar aided ICE-based CCHP system in office buildings under different operation strategies. The results indicated that the efficiency of the proposed system could get to 89% on a typical summer day, while the CO_2 emissions production of 2217 kg/day was reduced on a typical winter day. Lu and Wang [16] also proposed a

solar-assisted CCHP system using ICE as the PM and the impact of solar energy and thermal energy storage (TES) on the thermodynamic performance of CCHP was analyzed via a case study. Boyaghchi [17] proposed a novel micro solar hybrid CCHP system integrated with an organic Rankine cycle and it was analyzed via thermodynamic and thermo-economic methods in both typical summer and winter days. In addition, a TES was set to balance the supplied energy and demanded energy.

The abovementioned researchers prove the feasibility of a solar hybrid CCHP system and it is essential to further optimize the proposed system. However, the simulation work needs more computational work and it costs more time. Thus it is intensely necessary to select the optimum system parameters quickly and accurately using an optimization algorithm [18]. The majority of energy system optimization cases need to require the consideration of multiple objectives [17]. Ju et al. [19] proposed a multi-objective optimization method for a CCHP system to balance the results of different optimization modes. Wu et al. [20] built a multi-objective model for a micro-CCHP system to select the optimal running strategies and investigated the thermodynamic performance under different user demands. Also, Hu and Cho [21] proposed a random multi-objective optimization model to optimize the CCHP operation strategy. The probability constraints were introduced to make the running strategy more reliable. Abdollahi et al. [22] performed a multi-objective optimization for a small-scale CCHP system using energetic efficiency, total levelized cost rate, and thermos-economic as the objective functions.

The recent studies show that the researchers optimized the hybrid CCHP system with a selected PM. However, little public literature focuses its attention on the capacity selection of the PMs. Besides, in a solar hybrid CCHP system, the thermodynamic performance of the proposed system is exceedingly affected by the area of the solar field. In this study, a novel solar hybrid ICE-based CCHP system is proposed considering the part-load conditions of real PMs. Four selected scenarios of PMs have been investigated and the multi-objective models were performed to suggest both the proper scenario for building applications and the most appropriate number of collectors. Moreover, the thermodynamic performance of the proposed CCHP system is determined through a case study of a hotel.

2. System Description

The proposed solar hybrid ICE-based CCHP system including an ICE, parabolic trough collector (PTC), thermal energy storage (TES), boiler and absorption chiller. The system can provide cooling, heating and power to the nearby building.

The electricity is produced by the ICE and the operating strategy is followed by the FEL, because this running strategy consumes the minimum fossil fuel. If the maximum electricity produced by the CCHP system is less than the building demand, the additional power requirement is considered from the power grid. In addition, the waste heat of exhaust gas is further recovered for heating and cooling. However, the recovered thermal energy may not satisfy the energy requirement; therefore, the energy gap is considered from the PTC and the auxiliary boiler. The schematic of the proposed solar-assisted ICE-based CCHP system is illustrated in Fig. 1.

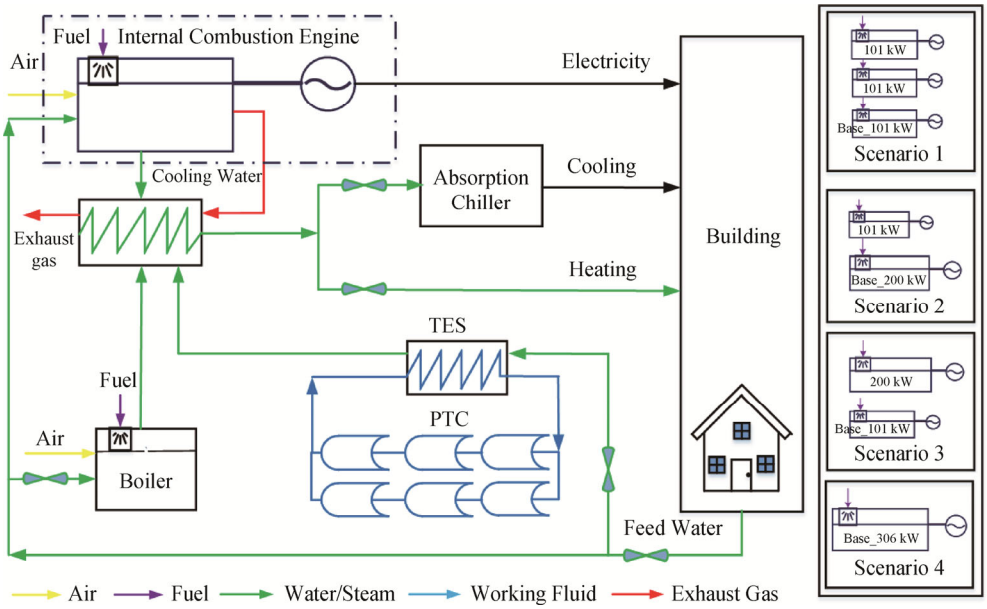

Fig. 1 Schematic of the proposed solar assisted ICE-based CCHP system

Additionally, the cooling and heating energy profiles are fulfilled by the waste heat of ICE, the energy from PTC, and the boiler. The type of the PTC is the LS-3, which has a larger aperture and a lower mirror cost per square meter than LS-2. The outlet temperature of the PTC can reach up to 400°C. In the daytime, the PTC collects solar energy for cooling/heating and stores extra energy in the TES. While on a cloudy day or at night, the TES releases the stored energy. The recovered heat will be changed with the variation of power loads and the direct normal irradiance (DNI). If the recovered thermal energy from ICE and PTC cannot satisfy the building demands, then the boiler will start.

Table 1 Technical specifications of the PMs

Technical specifications	Volve_101/ kW	Volve_200/ kW	Volve_306/ kW
Nominal capacity/ kW	101	200	306
Efficiency/%	91.5	92	92.5
Compression ratio	17.5	18.0	20.2
Speed/r·min^{-1}	1500	1500	1500
Voltage/V	230/240	230/240	230/240
Voltage regulation accuracy	+/–1.0%	+/–1.0%	+/–1.0%
Type of fuel	Natural gas	Natural gas	Natural gas
Cooling	Water/Air	Water/Air	Water/Air

For the cooling system, a single effect water-lithium bromide absorption chiller is selected and it is designed to operate in a range of hot water inlet temperatures between 75°C and 90°C [23]. The ICE is a natural gas-fueled PM made by Volvo Penta [24]. Additionally, the PM can be used by the different capacities of ICE and the scenarios of different capacities of ICEs impact the thermodynamic performance of the proposed CCHP. The technical specifications of PM are shown in Table 1.

3. Methodology

3.1 System formulation

The energy balance for the PM can be expressed as:

$$\dot{Q}_{\mathrm{PM}} = \dot{E}_{\mathrm{PM}} + \dot{Q}_{\mathrm{W}} + \dot{Q}_{\mathrm{L}} \tag{1}$$

where $\dot{E}_{\mathrm{PM}}$ is the electricity generated by the PM; $\dot{Q}_{\mathrm{PM}}$, $\dot{Q}_{\mathrm{W}}$, $\dot{Q}_{\mathrm{L}}$ is the energy released by the fuel combustion, recovered waste heat from PM and the energy loss. The $\dot{Q}_{\mathrm{PM}}$ can further be calculated by the fuel consumption rate of the PM ($\dot{m}_{\mathrm{f}}$) and the lower heating value of the fuel (LHV). The compositions of natural gas are list in Table 2.

$$\dot{Q}_{\mathrm{PM}} = \dot{m}_{\mathrm{f}} \times \mathrm{LHV} \tag{2}$$

Table 2 Parameters of selected PTC [25, 26]

Parameters	Values
Collector type	LS-3
Aperture width/m	5.75
Collector length/m	12
Aperture area/m^2	69
Optical efficiency/%	73.3
Mirror reflectance/%	94
Receiver absorptivity/%	96
PTC outlet temperature/°C	93
Maximum outlet temperature/°C	400
Row orientation	North-South
TES capacity/kW	4000

The power generation efficiency and the thermal efficiency of the PM can be defined as:

$$\eta_{\mathrm{PM}} = \dot{E}_{\mathrm{PM}} / \dot{Q}_{\mathrm{PM}} \tag{3}$$

$$\eta_{\mathrm{T}} = \left(\dot{E}_{\mathrm{PM}} + \dot{Q}_{\mathrm{W}}\right) / \dot{Q}_{\mathrm{PM}} \tag{4}$$

When the produced electricity from PM ($\dot{E}_{\mathrm{PM}}$) cannot satisfy the electricity demand ($\dot{E}_{\mathrm{B}}$), the extra electricity is considered from the power grid ($\dot{E}_{\mathrm{G}}$) and the electricity balance can be written as:

$$\dot{E}_{\mathrm{B}} = \dot{E}_{\mathrm{PM}} + \dot{E}_{\mathrm{G}} \tag{5}$$

In this proposed solar hybrid CCHP system, a PTC is used to collect solar energy. The incident solar energy ($\dot{Q}_{\mathrm{i}}$) can be calculated by the equation:

$$\dot{Q}_{\mathrm{i}} = A \times N \times \mathrm{DNI} \tag{6}$$

where A is the area of a single solar collector; N is the number of collectors; DNI is the direct normal irradiance of the solar energy. For the PTC, the absorbed solar energy ($\dot{Q}_{\mathrm{S}}$) can further be defined by:

$$\dot{Q}_{\mathrm{S}} = \eta_{\mathrm{PTC}} \times \dot{Q}_{\mathrm{i}} \times K(\theta) \tag{7}$$

where the η_{PTC} is the optical efficiency of the collector, which is defined as 73.3% [25]. The parameters of selected PTC are list in Table 2. Moreover, θ is the incident angle of solar energy and $K(\theta)$ is the incident angle modifier, which can be calculated by [27]:

$$K(\theta) = \cos\theta - 5.250\ 97\times10^{-4}\theta - 2.859\ 621\times10^{-5}\theta^2 \tag{8}$$

In this study, a single-effect absorption chiller is used to produce cooling for the building and the cooling output ($\dot{Q}_{\mathrm{C}}$) can be calculated by:

$$\dot{Q}_{\mathrm{C}} = \dot{Q}_{\mathrm{C}}^{\mathrm{r}} \cdot \mathrm{COP} \tag{9}$$

where $\dot{Q}_{\mathrm{C}}^{\mathrm{r}}$ is the recovered energy by the absorption chiller and the COP is the coefficient of performance which is assumed as 0.76 from previous literature [27].

For the TES, when the thermal energy produced by the PTC is more than the required energy, the excess energy

($\dot{Q}_{\mathrm{E}}$) is stored in the TES, the energy balance equation can be written as:

$$\dot{Q}_{\mathrm{C}}^{\mathrm{r}}+\dot{Q}_{\mathrm{H}}=\dot{Q}_{\mathrm{S}}+\dot{Q}_{\mathrm{W}}-\dot{Q}_{\mathrm{E}} \tag{10}$$

When the recovered waste energy from PM and produced energy from PTC cannot satisfy the profiles of cooling and heating, an auxiliary boiler is considered to start up. The capacity of the boiler is 500 kW; the boiler efficiency is 0.85, and the fuel of the boiler is natural gas. Additionally, the thermal energy produced by the auxiliary boiler ($\dot{Q}_{\mathrm{B}}$) can be calculated as:

$$\dot{Q}_{\mathrm{B}}=\eta_{\mathrm{B}}\times\dot{m}_{\mathrm{B}}\times\mathrm{LHV} \tag{11}$$

where η_{B} and $\dot{m}_{\mathrm{B}}$ stand for the boiler efficiency and the fuel consumption by the boiler, respectively. Herein, the energy balance equation can be written as:

$$\dot{Q}_{\mathrm{C}}^{\mathrm{r}}+\dot{Q}_{\mathrm{H}}=\dot{Q}_{\mathrm{TES}}+\dot{Q}_{\mathrm{W}}+\dot{Q}_{\mathrm{B}}+\dot{Q}_{\mathrm{PTC}} \tag{12}$$

where $\dot{Q}_{\mathrm{TES}}$ is the released energy from TES and $\dot{Q}_{\mathrm{PTC}}$ is the produced energy by PTC.

3.2 Optimization functions

Multi-objective optimization is used to achieve maximum efficiency of different CCHP plants [12]. In this study, four different capacities of PMs are proposed and compared to help the decision-making and to find the best PM for the proposed CCHP system. As the most important component in a CCHP, the performance of PM plays a decisive role in the overall plant. Additionally, the input and output parameters of PM also change with the forms of PM combinations. Table 3 shows the scenarios of PMs.

In scenario 1, three same types of ICE (Volve_101 kW) are selected as the PMs. One of them is set as the base engine, which is operating all the time. The rest two ICEs are auxiliary engines to fulfill the power load together and the total capacity is 303 kW. In scenario 2, a capacity of 101 kW ICE is considered as the base engine and the Volve_200 kW is the auxiliary engine. The total capacity is 301 kW. Similar to scenario 2, scenario 3 also has both Volve_101 kW and Volve_200 kW. However, the last one is considered as the base engine.

In the above scenarios, the power load is divided into two parts, i.e., the baseload part and peak load part. And each part has a special PM responsible for the power supply. When the building's power load is under the capacity of the baseload engine, the peak load engine should be shut down to save fossil fuel. Additionally, another advantage of these three scenarios is that the baseload engine could operate at its higher loads with higher thermal efficiency.

However, in scenario 4, a single capacity of 306 kW ICE is suggested as the PM for the proposed CCHP system. In this case, the PM should be operated on all the time. Herein, it should be noticed that in order to better compare the four scenarios, the other components like PTC, single effect LiBr-water absorption chiller and auxiliary boiler are similar apart from the difference of PMs.

In this study, three objective functions including the PESR, CESR, ATC are considered in the multi-objective optimization.

The PESR is used to measure the primary energy saving in the CCHP system compared to the conventional system [12]:

$$\mathrm{PESR}=\frac{\mathrm{PEC}_{\mathrm{con}}-\mathrm{PEC}_{\mathrm{CCHP}}}{\mathrm{PEC}_{\mathrm{con}}} \tag{13}$$

The CESR is modeled to evaluate the environmental performance of the proposed CCHP system, which is related to global warming [12]:

$$\mathrm{CESR}=\frac{\mathrm{CE}_{\mathrm{con}}-\mathrm{CE}_{\mathrm{CCHP}}}{\mathrm{CE}_{\mathrm{con}}} \tag{14}$$

The evaluation criterion of ATC can be defined as the ratio of the annual total cost difference between the conventional system and the proposed CCHP system [12].

$$\mathrm{ATC}=C_{\mathrm{INV}}+C_{\mathrm{O\&M}}+C_{\mathrm{F}} \tag{15}$$

where $C_{\mathrm{O\&M}}$ is the annual maintenance cost and C_{F} is the annual energy cost. C_{INV} is the annual capital cost, and it can further be calculated as:

$$C_{\mathrm{INV}}=\mathrm{CRF}\times\mathrm{INV} \tag{16}$$

where CRF is the capital recovery factor and INV is the total capital investment [12].

$$\mathrm{CRF}=\frac{i(1+i)^{n}}{(1+i)^{n}-1} \tag{17}$$

$$\mathrm{INV}=C_{\mathrm{PM}}+C_{\mathrm{PTC}}+C_{\mathrm{AC}}+C_{\mathrm{TES}}+C_{\mathrm{AB}} \tag{18}$$

where i and n are the interest rate and the service life of the proposed system, respectively. Herein, according to the previously published literature, i and n are defined as 4.9% and 20 years [28]. Moreover, the capital investment of the main components in the proposed CCHP system is list in Table 4.

Table 3 The scenarios of PMs

PM	Scenario 1	Scenario 2	Scenario 3	Scenario 4
Volve_101/kW	3×101	1×101 (Base engine)	1×101	–
Volve_200/kW	–	1×200	1×200 (Base engine)	–
Volve_306/kW	–	–	–	1×306
Total Capacity/kW	303	301	301	306

Table 4 The main capital cost of the components

Components	Purchase equipment cost	Ref.
Prime mover/USD	$C_{PM}=\dot{E}_{PM}\left[863.55-137\ln\left(\dot{E}_{PM}\right)\right]$	[29]
Absorption chiller/USD	$C_{AC}=\dot{W}_{AC}\left[482\left(\dot{W}_{AC}\right)^{-0.072\ 73}-159.7\right]$	[29]
Thermal energy storage/USD	$C_{TES}=65\times Q_{TES}$	[30]
Solar field/USD	$C_{PTC}=770\times A_{PTC}$	[31]
Auxiliary Boiler/USD	$C_{AB}=130.68\times Q_{AB}$	[32]

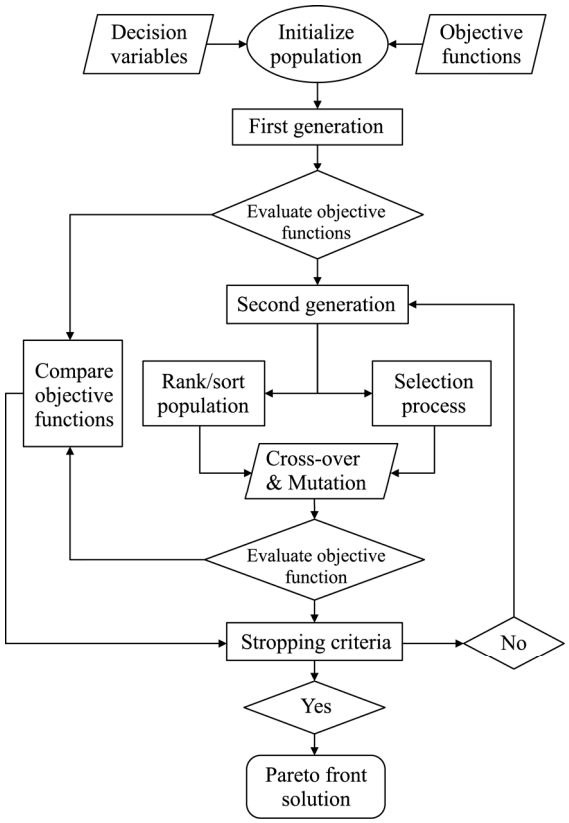

Fig. 2 The flow chart of the multi-objective genetic algorithm

Genetic algorithm (GA) is a search heuristic, based on techniques inspired by natural evolution, such as inheritance, mutation, selection, and crossover. The genetic algorithm process modifies the given population within the given logical bounds of the decision variables. In each step, the selected population is used as parents to produce children for the next generations. The population that has a higher fitness value is selected for the next iteration. This process continues until a set of the population is obtained which satisfies the objective function as well as the logical bound of the decision variables. The optimization was carried out in the MATLAB simulation environment. The layout of the multi-objective optimization is shown in Fig. 2.

4. Case Study

4.1 Building energy demands descriptions

In order to investigate the thermodynamic performance of the proposed solar hybrid CCHP system, a hotel is selected from previous work [18] as the case study. The hotel has seven floors with one basement: the roof area is 1478 m^2 and the total floor area is 11 345 m^2. In addition, the hourly energy demands of the hotel in typical summer, transition, and winter days are shown in Fig. 3. The reason why we select this hotel as the study case is that the energy output of the PM we selected can almost cover the energy demands of the hotel, and the user's energy demands change with the meteorological parameters. It's an ideal model to investigate the thermodynamic performance of the proposed CCHP system.

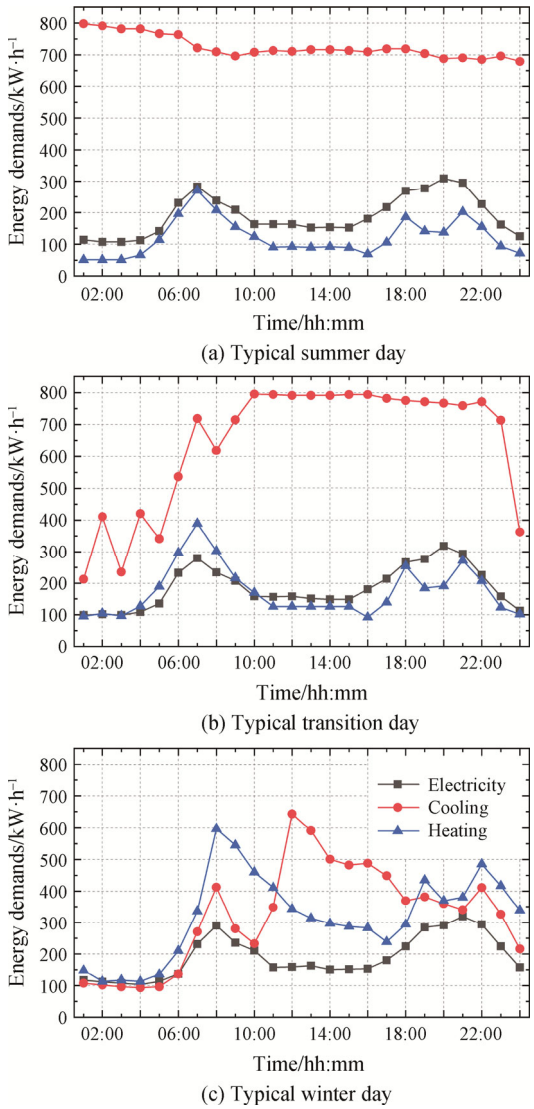

Fig. 3 Hourly energy demands of typical days

Shanghai is located at 121.47°E, 31.23°N, also on the west coast of the Pacific Ocean. Shanghai has a subtropical monsoon climate with distinct seasons and abundant sunshine. The typical weather data profiles (DNI and θ) are provided by the meteorological database.

4.2 Models validation

As the core engine in a CCHP system, the performance of PM has a great influence on the overall proposed system. In addition, because the PM runs under the part-load condition most of the time, the accuracy parameter of the model in part-load has a great influence on the economic analysis results of the system. The selected PMs in this study are modeled in the software Ebsilon Professional [33]. The designed values (Des_PM101, Des_PM200, and Des_PM306) from the manufacturer and the simulated results (Sim_PM101, Sim_PM200 and Sim_PM306) are shown in Fig. 4.

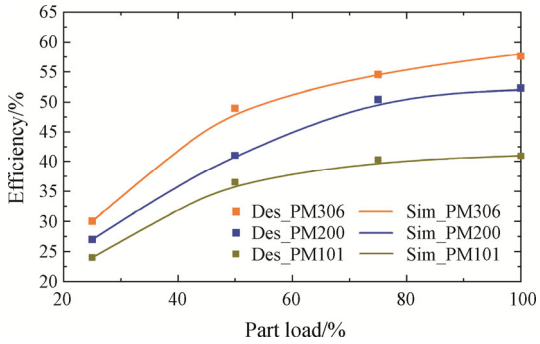

Fig. 4 Model validation by comparison with designed values

As can be seen, the values between designed and simulated show a good agreement. With such results, it is believed that the PM models are validated. Moreover, the parameters of PTC are obtained from Li and Yang [27], and the parameters of the absorption chiller are acquired by Wang et al. [26].

5. Results and Discussion

5.1 Optimization results

It is obvious that different seasons need a different number of collectors to cover the entire cooling and heating demands. In order to select the best PM, the yearly performance (ATC, CO_2 emissions, fuel cost, PESR and CESR) of each scenario with a different number of solar collectors (from 0 to 200) is calculated with MATLAB. Additionally, a hotel is considered as the case study to hourly evaluate the thermodynamic performance of proposed solar-assisted CCHP technology. For the PTC, a small area of solar field will not well reduce the primary energy consumption, while a large number of collectors will increase unnecessary initial investment. Therefore, it is extremely important to calculate a suitable number of collectors for users.

The fuel consumption and PTC investment under the different number of collectors are presented in Fig. 5. It can be seen that the PTC investment will increase linearly with the increasing area of the solar field. Moreover, the critical points (CPs) show the different needs for the typical summer, transition and winter days. A minimum collector number of 59 and a maximum collector number of 151 are required on a typical summer day and a typical winter day, respectively. The daily fuel consumption will drop dramatically with the increase of the number of collectors before the CP. However, after the CP, the daily fuel consumption will remain at a fixed value. For the reason that, after this point (CP), the collected solar thermal energy is larger than the required energy and the customers cannot consume the excess energy. However, for a certainty CCHP system, the number of collectors cannot be changed with the seasons and it should be determined at the design stage. Therefore, to select the right number of collectors for the proposed solar hybrid CCHP system, the optimization was carried out in the simulation environment of the multi-objective genetic algorithm in MATLAB. Under the logical bound of the number of solar collectors, the ATC was minimized while the CESR and PESR were maximized.

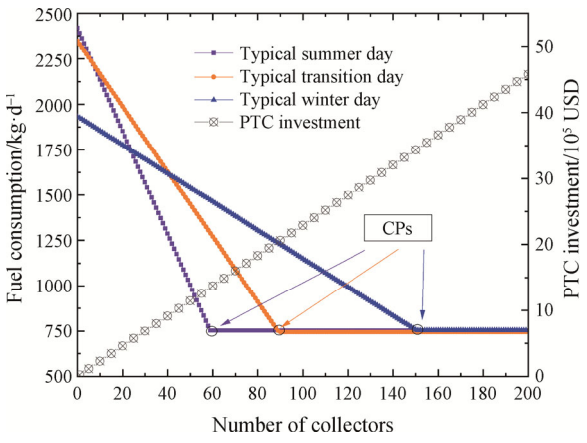

Fig. 5 Fuel consumption and PTC investment under the different number of collectors

The multi-objective optimization results are shown in Fig. 6. It can be seen that the increase in the number of solar collectors results in an increase in the cost of the CCHP system. There is a sharp decrease in fuel consumption and CO_2 emissions when the number of solar collectors is increased from 0 to 90. However, with the further increase in the number of solar collectors after 90, the decrease in fuel consumption and CO_2 emission is not significant.

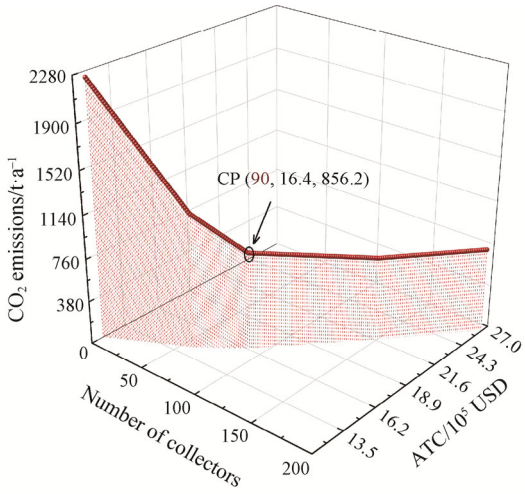

(a) CO_2 emissions and ATC change with the number of collectors

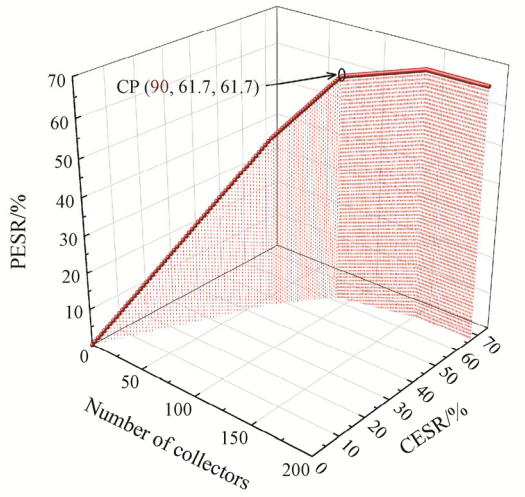

(b) PESR and CESR change with the number of collectors

Fig. 6 Pareto optimal frontier under the different number of collectors

Furthermore, the results of the multi-objective algorithm in terms of the decision variable and objective functions are shown in Fig. 6(b). When the number of collectors is increased from 0 to 90, the corresponding increase in the PESR and CESR is 61.61% respectively. The further increase in the number of solar collectors does not result in a noticeable increase in PESR and CESR. It can be seen from Fig. 6(a) and Fig. 6(b) that the optimum number of solar collectors is 90 for the considered CCHP system. Additionally, the collector number of 90 should be selected via the above multi-optimization to further evaluate the performance of the proposed CCHP system. The electricity load demands and supplied profiles from typical summer, transition and winter days are shown in Fig. 7. It can be seen that the peak power load occurs at 20:00 on both typical summer and transition days, while it appears at 21:00 on a typical winter day. Moreover, when the electrical loads are less than 306 kW, the selected PM can cover the power demands. However, if the power demands exceed the maximum capacity of PM (306 kW), the rest electricity is provided by the power grid. Besides, the profiles of the fuel consumption rate ($\dot{m}_f$) have a similar trend with the power output of PM.

Herein, it should be noticed that the operation strategy for the proposed CCHP system is under the FEL mode, which means that the power output of PM should be as consistent as possible with the electricity demand of the building. In addition, the advantage of this FEL mode is that it consumes less fossil fuel and the cooling/heating profiles are provided by recovered waste heat and solar energy, which does not require the consumption of fossil fuel. However, there is still a short period of time for the peak electricity load, thus selecting an appropriate

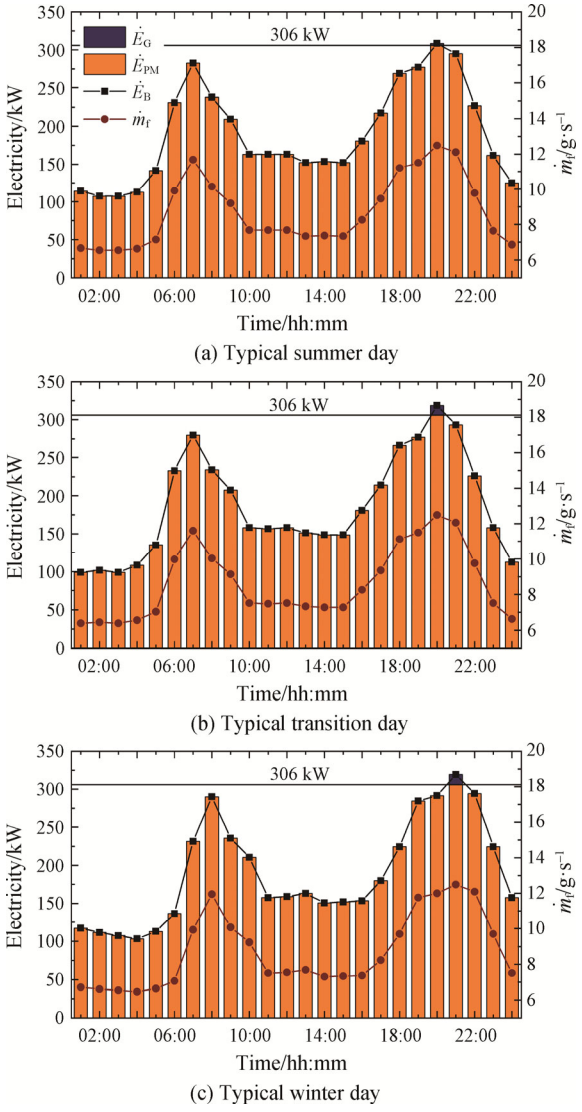

(a) Typical summer day

(b) Typical transition day

(c) Typical winter day

Fig. 7 Electricity load demands and supplied profiles from different typical days

capacity of PM can significantly avoid PM running under inefficient partial load for a long time.

The cooling load demands and supplied profiles from different typical days are depicted in Fig. 8. It can be seen that the cooling demands are supplied by the recovered waste heat from PM ($\dot{Q}_{\mathrm{W}}$), collected solar energy by PTC ($\dot{Q}_{\mathrm{S}}$), released energy from TES ($\dot{Q}_{\mathrm{TES}}$) and the auxiliary boiler ($\dot{Q}_{\mathrm{B}}$). When the total received energy by PM ($\dot{Q}_{\mathrm{W}}$) and PTC ($\dot{Q}_{\mathrm{S}}$) is larger than the required energy by cooling ($\dot{Q}_{\mathrm{C}}$) and heating ($\dot{Q}_{\mathrm{H}}$), a part of collected thermal energy by PTC will be stored in the TES (charging). Additionally, this part of stored thermal energy will be released during the cloudy day or at night (discharging).

In this proposed solar hybrid CCHP system, the selected area of PTC is large enough to supply the thermal energy for the building during sunny days. For a typical summer day shown in Fig. 8(a), the $\dot{Q}_{\mathrm{W}}$ provides 18.02% (3132.0 kW) of the overall energy demand; $\dot{Q}_{\mathrm{S}}$ and $\dot{Q}_{\mathrm{TES}}$ covers 36.06% (6266.0 kW) and 45.93% (7982.3 kW) of total cooling demands, respectively. While in transition and winter days, the auxiliary boiler is needed to produce extra energy for filling demands because both transition day and winter day have lower DNI than the summer day. In transition day, the percentage energy provided by $\dot{Q}_{\mathrm{W}}$, $\dot{Q}_{\mathrm{S}}$, $\dot{Q}_{\mathrm{TES}}$ and $\dot{Q}_{\mathrm{B}}$ are 18.39% (2844.7 kW), 37.66% (5825.1 kW), 42.18% (6524.5 kW) and 1.77% (274.4 kW). As for winter day, the percentage energy provided by $\dot{Q}_{\mathrm{W}}$, $\dot{Q}_{\mathrm{S}}$,

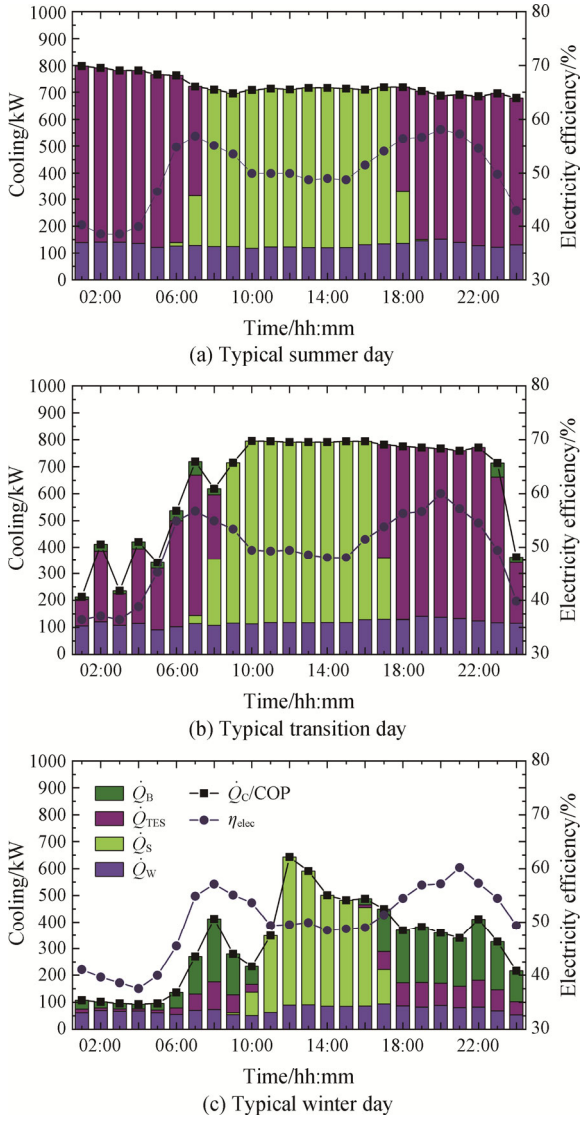

Fig. 8 Cooling load demands and supplied profiles from different typical days

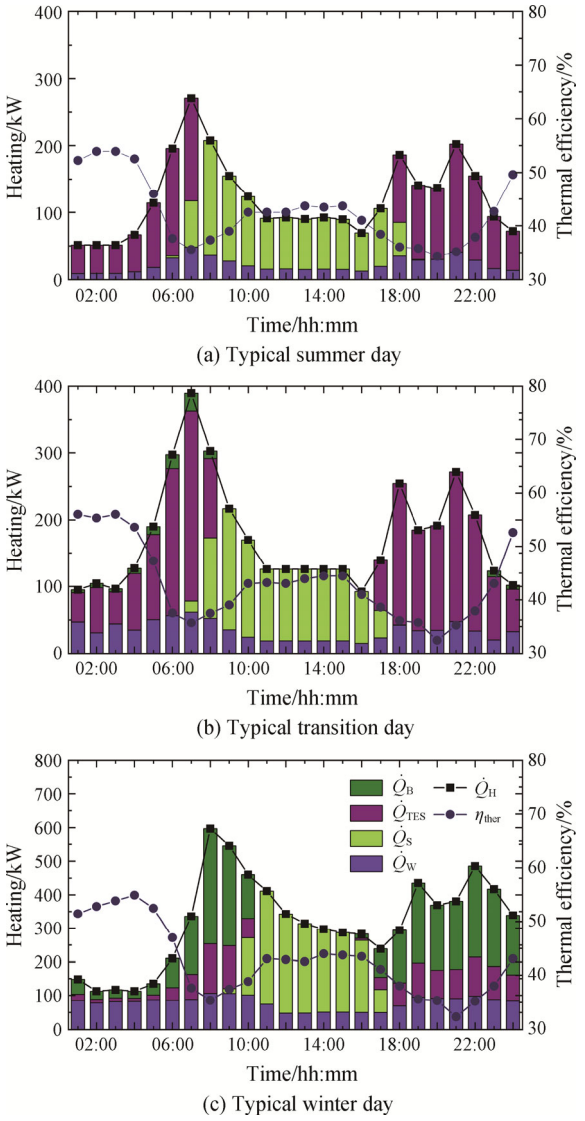

Fig. 9 Heating load demands and supplied profiles from different typical days

$\dot{Q}_{TES}$ and $\dot{Q}_B$ are 22.96% (1776.6 kW), 35.43% (2742.0 kW), 12.52% (968.6 kW) and 29.10% (2552.2 kW).

The heating load demands and supplied profiles from different typical days are presented in Fig. 9. It is illustrated that the heating demands are well fulfilled by the recovered waste heat from PM and the collected thermal energy by PTC in a typical summer day.

The percentage energy provided by $\dot{Q}_W$, $\dot{Q}_S$ and $\dot{Q}_{TES}$ on a typical summer day is 18.18% (528.4 kW), 35.96% (1045.5 kW), and 45.86% (1333.3 kW), respectively. While an auxiliary boiler is necessary to fulfill the energy gap in both typical transition days and typical winter days.

In winter, heating demand is much larger than in other seasons, for the winter has lower *DNI*, while buildings need extra thermal energy for space heating. In this study, the heating energy covered by $\dot{Q}_W$, $\dot{Q}_S$, $\dot{Q}_{TES}$ and $\dot{Q}_B$ are 24.64% (1890.3 kW), 24.08% (1847.3 kW), 15.42% (1183.4 kW) and 35.86% (2751.5 kW) on a typical winter day.

In addition, thermal efficiency has an opposite trend with electricity efficiency. For the reason that the PM with a lower power generation efficiency or a lower energy utilization releases more waste heat and this part of waste heat is recovered for further utilization, which promotes the improvement of thermal efficiency.

5.2 Sensitivity analysis

The fossil fuel price is different between countries and areas. Also, it will change with technology development and market influence in the same area. In this part, the sensitivity studies are performed to investigate the impact of the fuel price on the ATC and the dynamic investment payback period. The ATC changed with the number of collectors is illustrated in Fig. 10. It can be seen that the ATC will increase with the increase of the collector number and the benefits of the proposed CCHP system will be enhanced with a lower fuel price, for the reason that, in the proposed CCHP system, most part of the electricity is produced by the PM with fossil fuel and a lower fuel price will be better for customers.

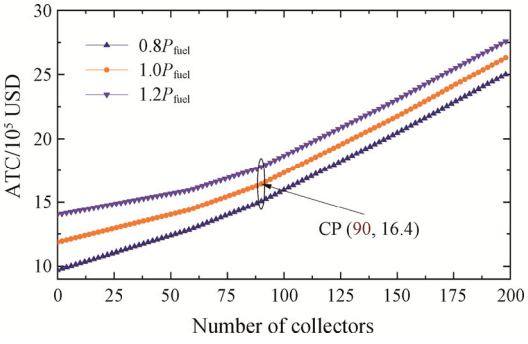

Fig. 10 The ATC changes with the number of collectors

The dynamic investment payback period changing with the number of collectors is performed in Fig. 11. It also can be concluded that the dynamic payback period drops rapidly before the CP (90). However, it will increase steadily after the CP, for the reason that the lower area of the solar field still has a large initial investment and the use of excessive solar collectors will cause serious energy waste, thus increasing the investment payback period. Herein, the investment payback period will change from 3.01 years to 3.56 years (under the collector number of 90) when the fuel price ranges from $0.8P_{fuel}$ to $1.2P_{fuel}$. In addition, the results of this sensitivity analysis can also verify the correctness of selecting the optimum number of collectors by multi-objective optimization.

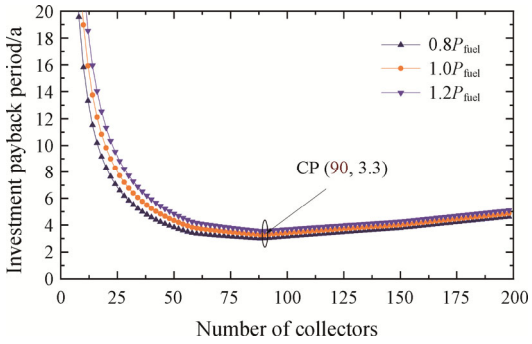

Fig. 11 Investment payback period changing with the number of collectors

6. Conclusions

The present study concerns analyzing a solar hybrid CCHP system driven by different capacities of PMs. The part-load performance of PMs is validated by the designed value from the manufacturer. Moreover, a multi-optimization model based on a genetic algorithm is developed in order to select both the most promising performance PM and the most cost-effectiveness, environmentally friendly number of collectors for the proposed CCHP system, simultaneously. Then the hourly performance of this solar hybrid CCHP is determined through a case study of a hotel in Shanghai. The following conclusions could be deduced:

(1) According to the multi-optimization, the highest efficiency of PM (scenario 4) with larger capacity had the most promising performance for building application due to its lower equipment investment for per kilowatt, higher electricity efficiency and excellent part-load performance compared with other scenarios.

(2) In the proposed solar hybrid CCHP system, the running strategy of the FEL model consumed less fossil fuel. In addition, the cooling/heating profiles were fulfilled by the recovered waste heat and solar energy.

(3) A proper initial investment will yield the highest returns. The collector number required ranged from 59 to 151 and the multi-optimization model significantly provided the optimal results for decision-making. In the case study, the most cost-effective, environmentally friendly solar collector number of 90 turns out to be a superior value for the hotel building.

(4) On a typical summer day, the recovered waste heat and solar energy can provide all the thermal energy demands (cooling and heating). For cooling demands, the proportion of energy provided by $\dot{Q}_{\mathrm{W}}$, $\dot{Q}_{\mathrm{S}}$ and $\dot{Q}_{\mathrm{TES}}$ are 18.02% (3132.0 kW), 36.06% (6266.0 kW) and 45.93 (7982.3 kW), respectively. While, for heating demands, the provided energy proportion is 18.18% (528.4 kW), 35.96% (1045.5 kW), and 45.86% (1333.3 kW), respectively.

(5) Both in typical winter and transition days, the auxiliary boiler should be started to fulfill the energy gap. In typical winter day, the covered cooling energy by $\dot{Q}_{\mathrm{W}}$, $\dot{Q}_{\mathrm{S}}$, $\dot{Q}_{\mathrm{TES}}$ and $\dot{Q}_{\mathrm{B}}$ are 22.96% (1776.6 kW), 35.43% (2742.0 kW), 12.52% (968.6 kW) and 29.10% (2552.2 kW), respectively. While, the provided heating energy are 24.64% (1890.3 kW), 24.08% (1847.3 kW), 15.42% (1183.4 kW) and 35.86% (2751.5 kW), respectively.

(6) The solar hybrid CCHP system has a promising performance in CO_2 emissions reduction. From the multi-optimization results, the system can reduce CO_2 emissions by 856.2 t/year, the value of CDSR can reach 61.7% due to the solar energy introduced into the system, thus slowing down global warming.

(7) From the sensitivity analysis, the ATC will increase with the increase of the collector number and the benefits of the system will be enhanced with a decrease in the fuel price. The dynamic investment payback period of the proposed solar hybrid CCHP system will range from 3.01 years to 3.56 years (under the collector number of 90) when the fuel price ranged from $0.8P_{\mathrm{fuel}}$ to $1.2P_{\mathrm{fuel}}$.

Acknowledgment

This research was financially supported by the Ph.D. research startup foundation of Northeast Electric Power University (BSJXM-2020209).

Conflict of Interest

On behalf of all authors, the corresponding author states that there is no conflict of interest.

References

[1] Hou Q., Zhao H., Yang X., Economic performance study of the integrated MR-SOFC-CCHP system. Energy, 2019, 166: 236–245.

[2] Vahid G., Hassan H., Mohammad S.D., Comparison of gas turbine and diesel engine in optimal design of CCHP plant integrated with multi-effect and reverse osmosis desalinations. Process Safety and Environmental Protection, 2021, 154: 505–518.

[3] Mahdi D-D., Marziye N., Sustainability assessment and emergy analysis of employing the CCHP system under two different scenarios in a data center. Renewable and sustainable Energy Reviews, 2021, 150: 111511.

[4] Ahn H., Freihaut J.D., Rim D., Economic feasibility of combined cooling, heating, and power (CCHP) systems considering electricity standby tariffs. Energy, 2019, 169: 420–432.

[5] Feng L., Dai X., Mo J., Ma Y., Shi L., Analysis of energy matching performance between CCHP systems and users based on different operation strategies. Energy Conversion and Management, 2019, 182: 60–71.

[6] Wang J.G., Hu X.M., BouDagher-Fadel M., Wu F.Y., Sun G.Y., Early Eocene sedimentary recycling in the Kailas area, southwestern Tibet: Implications for the initial India-Asia collision. Sedimentary Geology, 2015, 315: 1–13.

[7] Jia J.D., Chen H.W., Liu H.T., Ai T.C., Li H.Q., Thermodynamic performance analyses for CCHP system coupled with organic Rankine cycle and solar thermal utilization under a novel operation strategy. Energy Conversion and Management, 2021, 239: 114212.

[8] Ali T., Rahim K.S., Optimization of combined cooling, heating and power (CCHP) system with a gas turbine prime mover: A case study in the dairy industry. Energy, 2021, 229: 120788.

[9] Jiang R., Han W., Qin F., et al., Thermodynamic model development, experimental validation and performance analysis of a MW CCHP system integrated with dehumidification system. Energy Conversion and Management, 2018, 158: 176–185.

[10] Roman K., Alvey J., Selection of prime mover for combined cooling, heating, and power systems based on energy savings, life cycle analysis and environmental consideration. Energy and Buildings, 2016, 110: 170–181.

[11] Ebrahimi M., Keshavarz A., Prime mover selection for a residential micro-CCHP by using two multi-criteria decision-making methods. Energy and Buildings, 2012, 55: 322–331.

[12] Abbasi M., Sayyaadi H., Tahmasbzadebaie M., A methodology to obtain the foremost type and optimal size of the prime mover of a CCHP system for a large-scale residential application. Applied Thermal Engineering, 2018, 135: 389–405.

[13] Su B., Han W., Chen Y., Wang Z., Qu W., Jin H., Performance optimization of a solar assisted CCHP based

on biogas reforming. Energy Conversion and Management, 2018, 171: 604–617.

[14] Yousefi H., Ghodusinejad M., Kasaeian A., Multi-objective optimal component sizing of a hybrid ICE+PV/T driven CCHP microgrid. Applied Thermal Engineering, 2017, 122: 126–138.

[15] Fani M., Sadreddin A., Solar assisted CCHP system, energetic, economic and environmental analysis, case study: Educational office buildings. Energy and Buildings, 2017, 136: 100–109.

[16] Lu Y., Wang J., Thermodynamics performance analysis of solar-assisted combined cooling, heating and power system with thermal storage. Energy Procedia, 2017, 142: 3226–3233.

[17] Boyaghchi F., Heidarnejad P., Thermoeconomic assessment and multi objective optimization of a solar micro CCHP based on Organic Rankine Cycle for domestic application. Energy Conversion and Management, 2015, 97: 224–234.

[18] Yang G., Zhai X., Optimization and performance analysis of solar hybrid CCHP systems under different operation strategies. Applied Thermal Engineering, 2018, 133: 327–340.

[19] Ju L., Tan Z., Li H., Tan Q., Yu X., Song X., Multi-objective operation optimization and evaluation model for CCHP and renewable energy based hybrid energy system driven by distributed energy resources in China. Energy, 2016, 111: 322–340.

[20] Wu J., Wang J., Li S., Multi-objective optimal operation strategy study of micro-CCHP system. Energy, 2012, 48(1): 472–483.

[21] Hu M., Cho H., A probability constrained multi-objective optimization model for CCHP system operation decision support. Applied Energy, 2014, 116: 230–242.

[22] Abdollahi G., Sayyaadi H., Application of the multi-objective optimization and risk analysis for the sizing of a residential small-scale CCHP system. Energy and Buildings, 2013, 60: 330–344.

[23] Lubis A., Jeong J., Giannetti N., et al., Operation performance enhancement of single-double-effect absorption chiller. Applied Energy, 2018, 219: 299–311.

[24] https://www.volvopenta.com/.

[25] Li Y., Yang Y., Impacts of solar multiples on the performance of integrated solar combined cycle systems with two direct steam generation field. Applied Energy, 2015, 160: 673–680.

[26] Montes M., Abánades A., Martínez-Val J.M., et al., Solar multiple optimization for a solar-only thermal power plant, using oil as heat transfer fluid in the parabolic trough collectors. Solar Energy, 2009, 83: 2165–2176.

[27] Wang L., Lu J., Wang W., Ding J., Energy, environmental and economic evaluation of the CCHP systems for a remote island in south of China. Applied Energy, 2016, 183: 874–883.

[28] Li Y., Xiong Y., Thermo-economic analysis of a novel cascade integrated solar combined cycle system. Energy, 2018, 145: 116–127.

[29] Chen Y., Han W., Jin H., Investigation of an ammonia-water combined power and cooling system driven by the jacket water and exhaust gas heat of an internal combustion engine. International Journal of Refrigeration, 2017, 82: 174–188.

[30] Abbasi M., Chahartaghi M., Hashemian S., Energy, exergy, and economic evaluations of a CCHP system by using the internal combustion engines and gas turbine as prime movers. Energy Conversion and Management, 2018, 173: 359–374.

[31] Widyolar B., Jiang L., Winston R., Spectral beam splitting in hybrid PV/T parabolic trough systems for power generation. Applied Energy, 2018, 209: 236–250.

[32] Nezammahalleh H., Farhadi F., Tanhaemami M., Conceptual design and techno-economic assessment of integrated solar combined cycle system with DSG technology. Solar Energy, 2010, 84: 1696–1705.

[33] https://www.steag-systemtechnologies.com/en/products/ebsilon-professional/